Sample of a Good Lab Report

By Dr John Soo

The following is a sample lab report that I produced for my Year 2 physics laboratory back when I was studying at the National University of Singapore. I hope you do realize by now: a lab report is not as long as you think it is! This is probably not the best lab report out there, but I do expect you to produce something at least as good as this! :)

Absorption of Gamma and Beta Rays

John Soo Yue Han (A0074XXXX)

Abstract

In this experiment we study the absorption of gamma and beta rays by several kinds of materials. Using a Geiger counter and materials like plexiglass, aluminium and lead, we find that the impulse counting rate is inversely proportional to the square of the distance between the source material and the counter tube. The half-value thicknesses ($d_{1/2}$) of Plexiglass, concrete, aluminium, iron and lead are estimated to be 10 ± 1, 8.1 ± 0.1, 5.7 ± 0.7, 2.7 ± 0.3 and 1.28 ± 0.02 respectively; while the absorption coefficients (μ) for the respective materials are 0.07 ± 0.01, 0.086 ± 0.006, 0.12 ± 0.01, 0.26 ± 0.03 and 0.54 ± 0.01.

1. Theory

Gamma rays and beta particles are nuclear radioactive emissions. Gamma rays are electromagnetic radiations of high frequency which are naturally produced on Earth through the decay of high energy states in atomic nuclei. Beta particles on the other hand, are high speed electrons or positrons emitted by certain types of radioactive nuclei. Beta radiation has medium penetrating and ionising power, and can be stopped by a few millimetres of aluminium. Gamma rays have very high penetrating power, and can only be shielded off with thick amount of materials with high atomic number and density. **Fig. 1** shows a schematic diagram of the penetrability of beta and gamma rays.

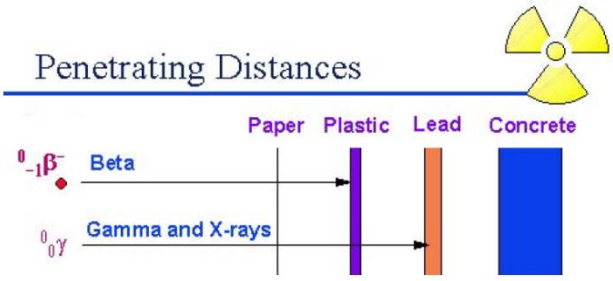

Fig. 1: Penetrating distances of beta and gamma rays.

The radioactivity of a substance can be measured by using a Geiger counter, connected to a detector tube. In studying these 2 kinds of radiation, we are especially interested in how the impulse counting rate ($\dot{N}$) will change with the distance from the counter tube (r). These 2 variables can be represented by the formula $\dot{N} = \frac{a}{r^2}$, where a is a constant.

The attenuation of the gamma rays or beta rays when they pass through an absorber of thickness d is expressed by the exponential law $\dot{N} = \dot{N}_0 e^{-\mu d}$, where $\dot{N}_0$ is the *impulse counting rate* when there is no absorber material, and it depends on the energy of the gamma quantum.

The variable μ is the *absorption coefficient* of a certain material, which is proportional to the number of electrons in the shell per unit volume, or approximately proportional to the density (ρ) of the material. With this value, we could obtain the half-value thickness of a material ($d_{1/2}$), which is the thickness at which the impulse counting rate is reduced by half. This value is represented by the equation $d_{1/2} = \frac{\ln 2}{\mu}$.

The **aim of this experiment** is to understand the interaction of radiation and matter, and the application to radiation detecting and shielding. In this experiment, we will find

a. The relationship between the impulse counting rate and the distance between the source and the counter tube; and
b. The half-value thickness ($d_{1/2}$) and the absorption coefficient (μ) of Plexiglass, concrete, aluminium, iron and lead.

2. Experiment

Fig. 2: Experimental setup for the absorption of gamma and beta rays.

The apparatus is set up as shown in **Fig. 2**. The Geiger tube detector is mounted on a holder, and is made to face the radioactive source Cobalt-60 (^{60}C) directly. The experiment is started with a background count for one minute, in which the counts are accounted by the cosmic rays and radioactive materials present in the ground and the building. This count is denoted by $\dot{N}_B$. For part A, the source is placed 4 cm away from the detector. The counter is then set to measure the amount of counts received in one minute ($\dot{N}$). A total of 6 readings are taken, and the average reading is calculated. The experiment is repeated for distances 5 cm, 6 cm, 7 cm, 8 cm and 9 cm. A linear least-squares-fit and a graph of $\ln(\dot{N} - \dot{N}_B)$ against $\ln r$ is plotted, and the inverse square law is to be verified.

In Part B, the experiment is first started by testing the amount of aluminum absorbers required to shield off the beta rays from being counted by the tube detector. This is done by inserting sheets of aluminium between the detector and the source, measure the count rate, and slowly increasing the number of sheets and remeasure until the count rate reaches a fairly constant value. The thickness of a block of Plexiglass is measured using a micrometer screw gauge, and it is placed together with the amount of aluminium sheets required to shield the beta rays earlier, in between the detector and the ^{60}C source, which are 4 cm away from each other. The count rate for one minute is measured. The thickness of Plexiglass is slowly increased by inserting a few more blocks, and the count rate per minute is measured again each time. The experiment is repeated for blocks of concrete, aluminium, iron and lead. For each measurement, 6 readings are taken, and the average is calculated. A linear least-squares-fit and a graph of $\ln(\dot{N} - \dot{N}_B)$ against d is plotted, the absorption coefficient μ and half-value thickness $d_{1/2}$ for each material is calculated.

3. Results

PART A

The data collected for this experiment are attached in the Appendix. Based on the tables shown, the background count $\dot{N}_B$ is calculated to be 31 ± 4 counts per minute. With the background count measured, the graph of $\ln(\dot{N} - \dot{N}_B)$ against $\ln r$ is plotted and is shown in **Fig. 3** below.

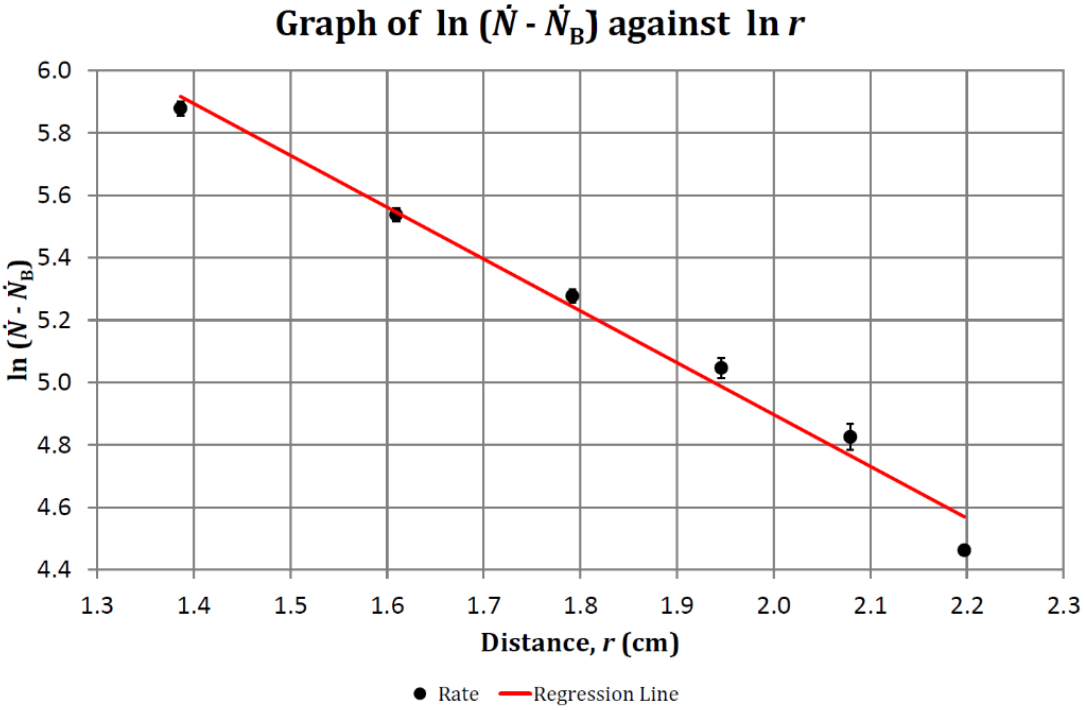

Fig. 3: Graph of $\ln(\dot{N} - \dot{N}_B)$ against $\ln r$.

Modifying the equation $\dot{N} = \frac{a}{r^2}$, we have $\ln \dot{N} = -2 \ln r + \ln a$, which is the equation of the line plotted. **Fig. 3** shows a gradient of $\mathbf{-1.7 \pm 0.1}$, a y-intercept of $\mathbf{8.2 \pm 0.2}$, and a correlation coefficient of **0.9833**. This shows that there is quite strong positive correlation between both the variables. Comparing with the equation derived, the gradient of the graph is equal to the theoretical value -2 within **15%** experimental uncertainty.

PART B

As per the previous part, the data collected are attached in the appendix for reference. From the beta particle shielding test, it shows that when we use aluminium sheets of thicknesses between 0.110 cm to 0.750 cm, the count rate is quite constant, and the count rate decreases drastically when the thickness of 0.925 cm is used. Therefore we made use of aluminium sheets of thickness **0.750 cm** to shield the beta particles in the next few parts of the experiment.

Modifying the equation $\dot{N} = \dot{N}_0 e^{-\mu d}$ to express it as $\ln \dot{N} = -\mu d + \ln \dot{N}_0$, we see that the term $-\mu$ is the gradient of a graph of $\ln \dot{N}$ against d. The graphs for Plexiglass, concrete, aluminium, iron and lead are plotted as shown in **Figs. 4** to **8**.

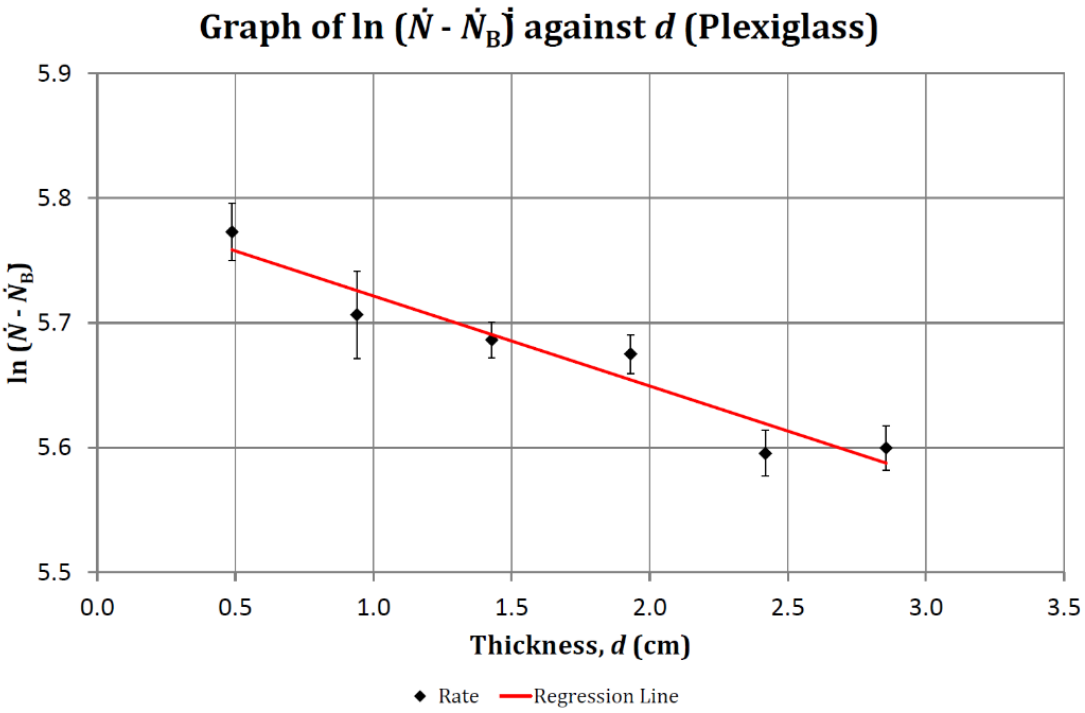

Fig. 4: Graph of $\ln(\dot{N} - \dot{N}_B)$ against the thickness of plexiglass.

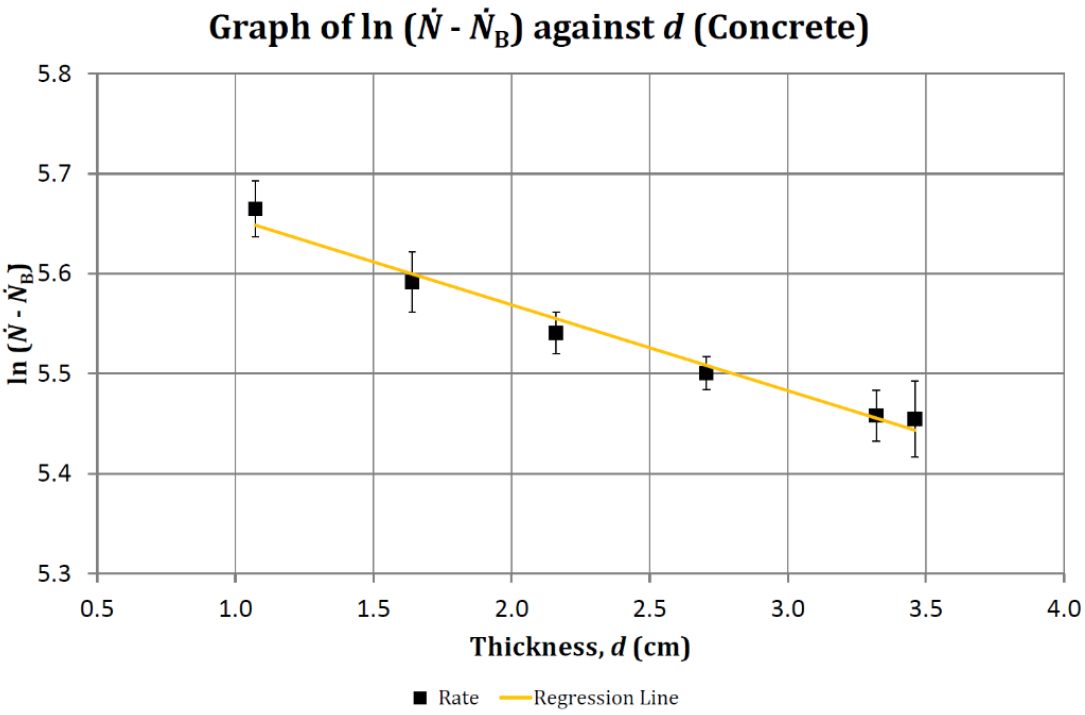

Fig. 5: Graph of $\ln(\dot{N} - \dot{N}_B)$ against the thickness of concret.

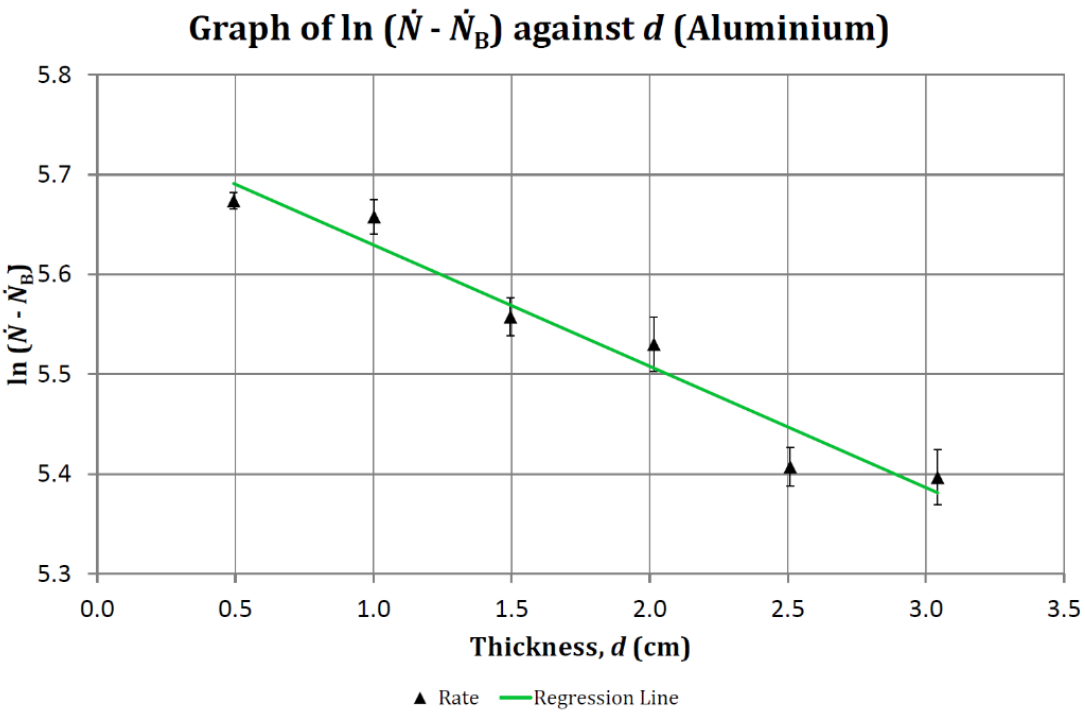

Fig. 6: Graph of $\ln(\dot{N} - \dot{N}_B)$ against the thickness of aluminium.

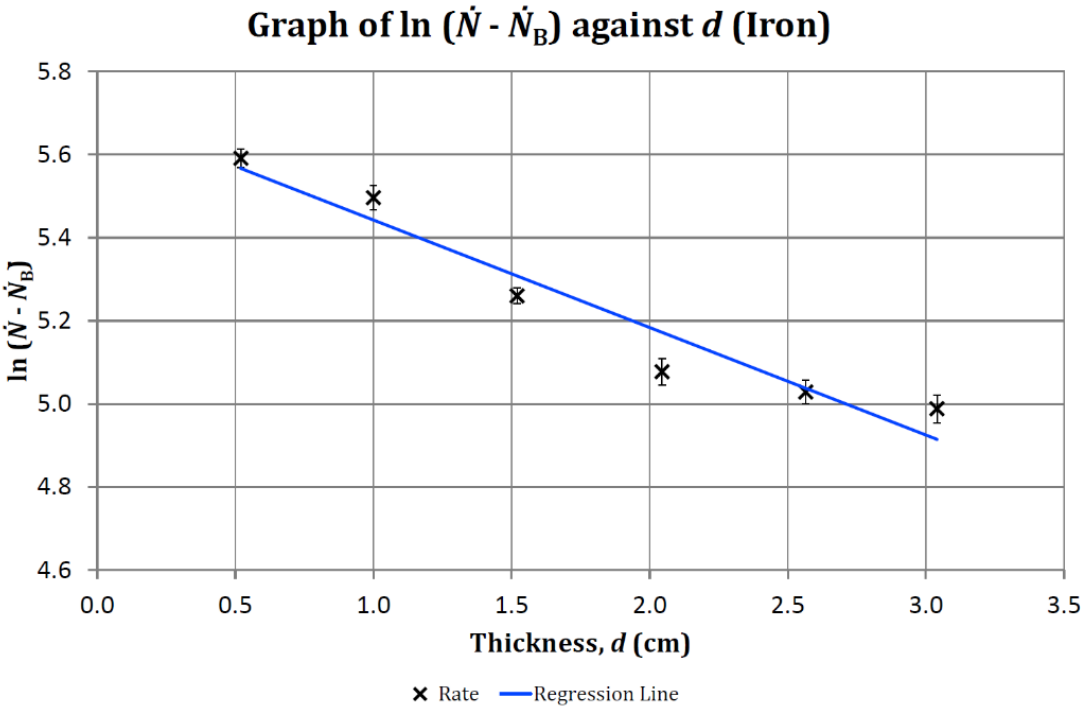

Fig. 7: Graph of $\ln(\dot{N} - \dot{N}_B)$ against the thickness of iron.

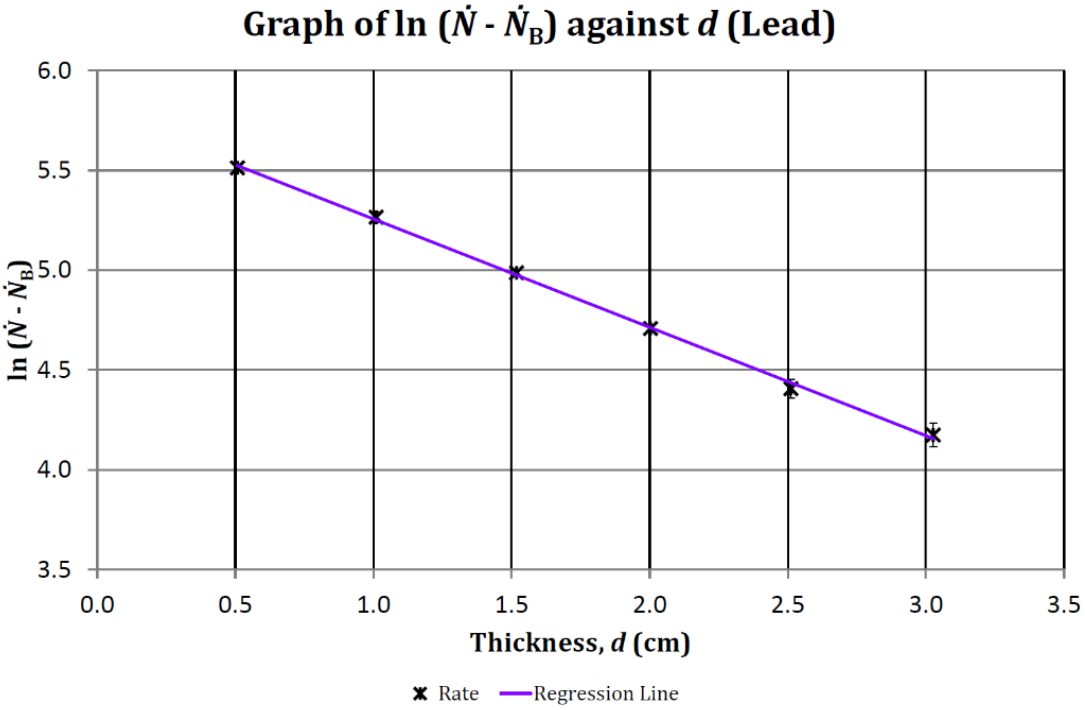

Fig. 8: Graph of $\ln(\dot{N} - \dot{N}_B)$ against the thickness of lead.

We further summarise all the graphs shown earlier in **Fig. 9** below.

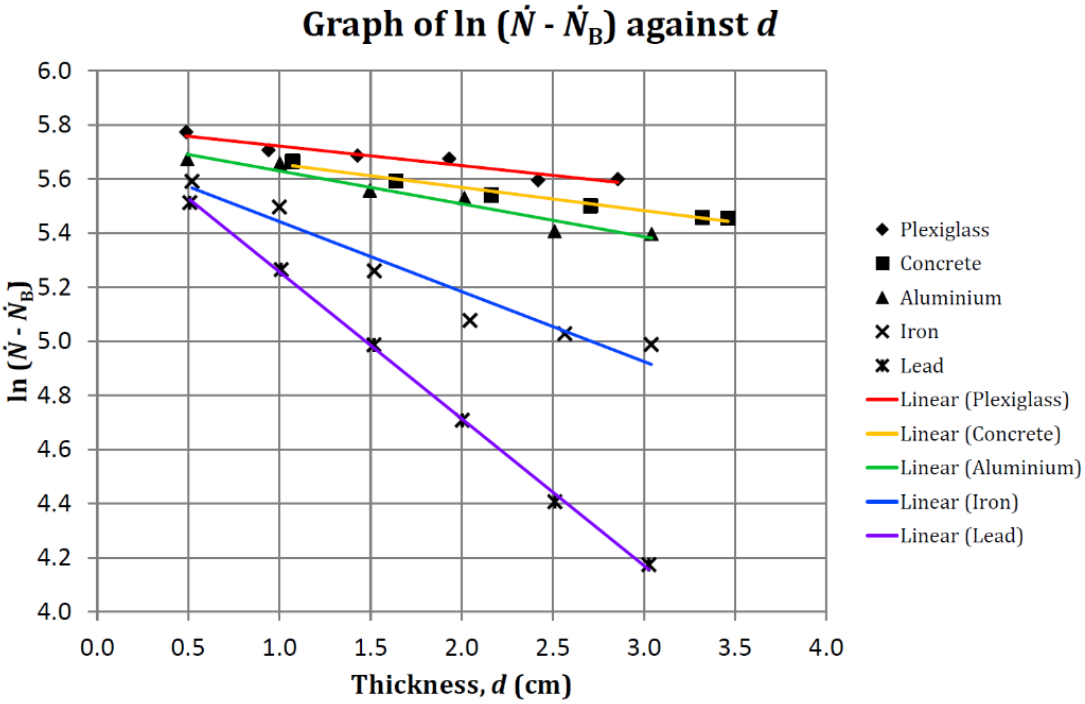

Fig. 9: A summary graph of $\ln(\dot{N} - \dot{N}_B)$ against the thicknesses of the materials used in this experiment.

The data collected from all the graphs in part B is summarized in **Table 1**.

Material	Gradient, m (cm^{-1})	y-intercept, c	Correlation Coefficient, r
Plexiglass	-0.07 ± 0.01	5.79 ± 0.02	0.9234
Concrete	-0.086 ± 0.006	5.74 ± 0.02	0.9784
Aluminium	-0.12 ± 0.01	5.75 ± 0.03	0.9493
Iron	-0.26 ± 0.03	5.70 ± 0.07	0.9374
Lead	-0.54 ± 0.01	5.80 ± 0.02	0.9987

Table 1: Data obtained from graphs plotted as shown in **Figs. 4** to **8**.

From the data obtained above, we see that every graph has a correlation coefficient of at least 0.9200 and above. This shows that there is quite strong positive correlation between the variables, and the equation is well verified. Using the fact that the gradient $m = -\mu$, and $d_{1/2} = \frac{\ln 2}{\mu}$, we thus summarize our final values of absorption coefficients and half-value thicknesses together with their percentage discrepancies in **Table 2** below.

Material	Absorption Coefficient, μ (cm^{-1})	Discr.	Half-value Thickness, $d_{1/2}$ (cm)	Discr.
Plexiglass	0.07 ± 0.01	7.4%	10 ± 1	7.9%
Concrete	0.086 ± 0.006	30.7%	8.1 ± 0.1	44.1%
Aluminium	0.12 ± 0.01	18.9%	5.7 ± 0.7	23.9%
Iron	0.26 ± 0.03	34.3%	2.7 ± 0.3	52.2%
Lead	0.54 ± 0.01	12.4%	1.28 ± 0.02	14.0%

Table 2: Calculated values of the absorption coefficient and half-value thickness for the respective materials.

4. Discussion

The errors for the measurements taken for a dependent variable y is based on the formula of propagation of errors,

$$\delta y = \sqrt{\left(\frac{\partial y}{\partial x_1}\delta x_1\right)^2 + \left(\frac{\partial y}{\partial x_2}\delta x_2\right)^2 + \cdots + \left(\frac{\partial y}{\partial x_n}\delta x_n\right)^2}$$

where $1,2,\ldots,n$ denote the number of independent variables. The error for gradients and y-intercepts of the graphs are calculated using Microsoft Excel using the formula

$$\delta m = \sqrt{\frac{N}{N\Sigma x^2 - (\Sigma x)^2}}\delta y, \qquad \delta c = \sqrt{\frac{\Sigma x^2}{N\Sigma x^2 - (\Sigma x)^2}}\delta y$$

which were taken from statistical theories. Using these equations, we calculated the errors in Part B for μ and $d_{1/2}$ to be $\delta\mu = \delta m$ and $\delta d_{1/2} = \frac{\ln 2}{\mu^2}\delta\mu$.

The data in this experiment have very high uncertainties and errors, and very low precisions (low percentage uncertainties) as well. This is because radioactivity is a random and spontaneous process, and one has to take many readings for every value (more than 10) and average them out to get a fairly good result. Since this is so, we can say that the high correlation coefficient of lead (0.9987), its low percentage uncertainty of μ (1.9%), the low percentage discrepancy of μ and $d_{1/2}$ for Plexigalss (7.4% and 7.9%) and etc do not mean that the characteristics of that particular material has influenced the results of the experiment.

Bringing the results one step further, we could also find the value of the constant a in the equation $\dot{N} = \frac{a}{r^2}$. We find that c, the y-intercept of the graph in part A, can be expressed as $c = \ln a$, and therefore, $a = e^c = (3.7 \pm 0.7) \times 10^3 \text{cm}^2$, which is quite a huge number. Further experiments can be conducted to determine whether this constant depends on any other parameters too. In a similar manner, the value of the mass attenuation coefficient μ/ρ, where ρ is the density of the material could also be found through the data from Part B. Finally, $\dot{N}_0$, the initial count rate when no absorbing material, can be extracted experimentally from part B. We know that the y-intercept, $c = \ln \dot{N}_0$, and therefore we find $\dot{N}_0$ averaged from these 5 graphs to be 316 ± 5 counts per minute. Compare this value to the data from part A (357 counts per minute for $r = 4$ cm), these two values have a percentage difference of 6.1%, which shows that these 2 experiments are equal within 6.1% experiment uncertainty.

5. Conclusion

From this experiment, we conclude that the impulse counting rate of the Geiger Counter is inversely proportional to the square of the distance between the source and the counter tube, within 15% experimental uncertainty.

We also conclude that the half-value thicknesses ($d_{1/2}$) of Plexiglass, concrete, aluminium, iron and lead are estimated to be 10 ± 1, 8.1 ± 0.1, 5.7 ± 0.7, 2.7 ± 0.3 and 1.28 ± 0.02 respectively; while the absorption coefficients (μ) for the respective materials are 0.07 ± 0.01, 0.086 ± 0.006, 0.12 ± 0.01, 0.26 ± 0.03 and 0.54 ± 0.01.

6. References

National University of Singapore (n. d.). *PC2193 Experimental Physics I Lab Manual*.

Fowler, M. (n. d.). *Rays and Particles.* Retrieved from http://galileo.phys.virginia.edu/classes/252/rays_and_particles.html on 27 Oct 2021.

United States Nuclear Regulatory Commission (2020). *Radiation* Basics. Retrieved from https://www.nrc.gov/about-nrc/radiation/health-effects/radiation-basics.html on 27 Oct 2021.

APPENDIX: Data collected for the experiment Absorption of Beta and Gamma Rays

PART A

Background Count

$\dot{N}_{B,1}$	$\dot{N}_{B,2}$	$\dot{N}_{B,3}$	$\dot{N}_{B,4}$	$\dot{N}_{B,5}$	$\dot{N}_{B,6}$	$\dot{N}_B$	$\delta\dot{N}_B$
20	29	23	25	42	47	31	4

Rate v.s. Distance

$\dot{N}_1$	$\dot{N}_2$	$\dot{N}_3$	$\dot{N}_4$	$\dot{N}_5$	$\dot{N}_6$	$\dot{N}$	$\delta\dot{N}$	r (cm)	ln r	$\dot{N}$-$\dot{N}_B$	ln ($\dot{N}$-$\dot{N}_B$)	y_{best}	δ(ln $\dot{N}$)
418	357	403	392	373	387	388	9	4.0	1.4	357	5.88	5.92	0.02
290	292	274	308	266	280	285	6	5.0	1.6	254	5.54	5.55	0.02
237	244	223	224	219	214	227	5	6.0	1.8	196	5.28	5.24	0.02
176	174	178	184	212	195	187	6	7.0	1.9	156	5.05	4.99	0.03
144	131	172	165	169	153	156	7	8.0	2.1	125	4.83	4.77	0.04
114	120	116	120	115	121	118	1	9.0	2.2	87	4.46	4.57	0.01

LINEST()			
m	-1.7	8.2	c
s_m	0.1	0.2	s_c
r	0.9833	0.07	s_y

PART B

Beta Ray Shielding Test

$\dot{N}_1$	$\dot{N}_2$	$\dot{N}_3$	$\dot{N}_4$	$\dot{N}_5$	$\dot{N}_6$	$\dot{N}$	$\delta\dot{N}$	d (cm)
298	344	340	327	323	366	333	9	0.110
346	332	351	320	318	343	335	6	0.346
345	322	320	305	329	333	326	6	0.580
341	342	306	349	344	328	335	6	0.710
327	318	296	313	328	297	313	6	0.925

r (cm)
4

Plexiglass

$\dot{N}_1$	$\dot{N}_2$	$\dot{N}_3$	$\dot{N}_4$	$\dot{N}_5$	$\dot{N}_6$	$\dot{N}$	$\delta\dot{N}$	d (cm)
378	344	348	334	335	376	353	8	0.488
340	330	280	329	349	363	332	12	0.940
311	343	334	317	324	326	326	5	1.428
309	341	321	311	332	321	323	5	1.931
305	274	303	300	306	313	300	6	2.419
310	302	299	307	313	277	301	5	2.856

$\dot{N}$-$\dot{N}_B$	ln ($\dot{N}$-$\dot{N}_B$)	y_{best}	δ ln ($\dot{N}$-$\dot{N}_B$)
322	5.77	5.76	0.02
301	5.71	5.73	0.03
295	5.69	5.69	0.01
292	5.68	5.65	0.02
269	5.60	5.62	0.02
270	5.60	5.59	0.02

LINEST()			
m	-0.07	5.79	c
s_m	0.01	0.02	s_c
r	0.9234	0.02	s_y

μ	0.07	$\delta\mu$	0.01	% discr	7.4
$d_{1/2}$	10	$\delta d_{1/2}$	1	% discr	7.9

Concrete

$\dot{N}_1$	$\dot{N}_2$	$\dot{N}_3$	$\dot{N}_4$	$\dot{N}_5$	$\dot{N}_6$	$\dot{N}$	$\delta\dot{N}$	d (cm)
321	322	283	346	335	310	320	9	1.073
292	275	293	323	282	330	299	9	1.640
304	272	284	290	298	267	286	6	2.162
290	259	285	270	273	278	276	5	2.706
288	247	262	284	254	259	266	7	3.320
256	227	265	272	304	265	265	10	3.460

$\dot{N}$-$\dot{N}_B$	ln ($\dot{N}$-$\dot{N}_B$)	y_{best}	δ ln ($\dot{N}$-$\dot{N}_B$)
289	5.66	5.65	0.03
268	5.59	5.60	0.03
255	5.54	5.55	0.02
245	5.50	5.51	0.02
235	5.46	5.46	0.03
234	5.45	5.44	0.04

LINEST()			
m	-0.086	5.74	c
s_m	0.006	0.02	s_c
r	0.9784	0.01	s_y

μ	0.086	$\delta\mu$	0.006	% discr	30.7
$d_{1/2}$	8.1	$\delta d_{1/2}$	0.6	% discr	44.1

Aluminium

$\dot{N}_1$	$\dot{N}_2$	$\dot{N}_3$	$\dot{N}_4$	$\dot{N}_5$	$\dot{N}_6$	$\dot{N}$	$\delta\dot{N}$	d (cm)
317	318	322	328	316	332	322	3	0.494
295	320	336	320	322	312	318	6	1.002
293	296	299	274	273	306	290	6	1.496
271	280	271	276	280	321	283	8	2.015
244	255	238	255	260	272	254	5	2.509
267	232	267	232	265	247	252	7	3.042

$\dot{N}$-$\dot{N}_B$	ln ($\dot{N}$-$\dot{N}_B$)	y_{best}	δ ln ($\dot{N}$-$\dot{N}_B$)
291	5.67	5.69	0.01
287	5.66	5.63	0.02
259	5.56	5.57	0.02
252	5.53	5.51	0.03
223	5.41	5.45	0.02
221	5.40	5.38	0.03

LINEST()			
m	-0.12	5.75	c
s_m	0.01	0.03	s_c
r	0.9493	0.03	s_y

μ	0.12	$\delta\mu$	0.01	% discr	18.9
$d_{1/2}$	5.7	$\delta d_{1/2}$	0.7	% discr	23.9

Iron

$\dot{N}_1$	$\dot{N}_2$	$\dot{N}_3$	$\dot{N}_4$	$\dot{N}_5$	$\dot{N}_6$	$\dot{N}$	$\delta\dot{N}$	d (cm)
273	296	297	312	294	322	299	7	0.520
255	289	282	245	294	284	275	8	1.000
223	228	210	234	233	213	224	4	1.520
206	175	183	189	213	182	191	6	2.045
190	196	187	175	162	192	184	5	2.565
195	167	181	156	176	191	178	6	3.040

$\dot{N}$-$\dot{N}_B$	ln ($\dot{N}$-$\dot{N}_B$)	y_{best}	δ ln ($\dot{N}$-$\dot{N}_B$)
268	5.59	5.57	0.02
244	5.50	5.44	0.03
193	5.26	5.31	0.02
160	5.08	5.17	0.03
153	5.03	5.04	0.03
147	4.99	4.91	0.03

LINEST()			
m	-0.26	5.70	c
s_m	0.03	0.07	s_c
r	0.9374	0.07	s_y

μ	0.26	$\delta\mu$	0.03	% discr	34.3
$d_{1/2}$	2.7	$\delta d_{1/2}$	0.3	% discr	52.2

Lead

$\dot{N}_1$	$\dot{N}_2$	$\dot{N}_3$	$\dot{N}_4$	$\dot{N}_5$	$\dot{N}_6$	$\dot{N}$	$\delta\dot{N}$	d (cm)
292	267	274	287	287	266	279	5	0.508
229	199	228	224	220	247	225	6	1.010
172	181	175	178	172	187	178	2	1.518
147	133	135	146	147	143	142	3	2.003
127	117	109	118	118	89	113	5	2.511
73	103	115	99	96	90	96	6	3.027

$\dot{N}$-$\dot{N}_B$	ln ($\dot{N}$-$\dot{N}_B$)	y_{best}	δ ln ($\dot{N}$-$\dot{N}_B$)
248	5.51	5.52	0.02
194	5.27	5.25	0.03
147	4.99	4.98	0.01
111	4.71	4.71	0.02
82	4.41	4.44	0.05
65	4.17	4.16	0.06

LINEST()			
m	-0.54	5.80	c
s_m	0.01	0.02	s_c
r	0.9987	0.02	s_y

μ	0.54	$\delta\mu$	0.01	% discr	12.4
$d_{1/2}$	1.28	$\delta d_{1/2}$	0.02	% discr	14.0